J|A|C|S ARTICLES

Published on Web 08/06/2009

Characterization of the Proximal Ligand in the P420 Form of Inducible Nitric Oxide Synthase

Joseph Sabat,[†] Dennis J. Stuehr,[‡] Syun-Ru Yeh,*[,†] and Denis L. Rousseau*[,†]

Department of Physiology and Biophysics, Albert Einstein College of Medicine, Bronx, New York 10461, and Department of Immunology, NN-l, The Cleveland Clinic, Cleveland, Ohio 44195

Received February 9, 2009; E-mail: syeh@aecom.yu.edu; rousseau@aecom.yu.edu

Abstract: The nitric oxide (NO) produced by inducible nitric oxide synthase (iNOS) up-regulates the expression of heme oxygenase (HO), which in turn produces carbon monoxide (CO) that down-regulates iNOS activity by reducing its expression level or by inhibiting its activity by converting it to an inactive P420 form ($iNOS_{P420}$). Accordingly, CO has been considered as a potentially important attenuator of inflammation. Despite its importance, the nature of the proximal heme ligand of the $iNOS_{P420}$ species remains elusive. Here we show that the 221 cm^{-1} mode of the photoproduct of $iNOS_{P420}$ does not exhibit any H_2O-D_2O solvent isotope shift such as that found in the iron−histidine stretching mode of myoglobin, indicating that the proximal ligand of $iNOS_{P420}$ is not a histidine. The ν_{Fe-CO} and ν_{C-O} data reveal that the proximal heme ligand of $iNOS_{P420}$ is consistent with a protonated thiol instead of a thiolate anion. Furthermore, the optical absorption properties of $iNOS_{P420}$ are similar to those of a neutral thiol−heme model complex but not myoglobin. Together the data support the scenario that $iNOS_{P420}$ is inactivated by protonation of the native proximal thiolate ligand to a neutral thiol, instead of by ligand switching to a histidine, as prior studies have suggested.

Introduction

Nitric oxide synthase (NOS) catalyzes the formation of nitric oxide (NO) from L-arginine (L-Arg) and two molecules of dioxygen in two successive monooxygenation reactions. The first reaction produces *N*-hydroxy-L-arginine (NOHA) and the second reaction produces L-citrulline and NO.[1−4] NOS is a homodimeric heme-containing enzyme. Each monomer is composed of an oxygenase domain, which binds the heme prosthetic group, the substrate, and the tetrahydrobiopterin (H_4B) cofactor, and a reductase domain, which binds flavin mononucleotide (FMN), flavin adenine dinucleotide (FAD), and reduced nicotinamide adenine dinucleotide phosphate (NADPH).[5,6] Electron transfer from the reductase domain to the oxygenase domain, required for the oxygen chemistry, is enabled by the binding of calmodulin in the interface between the two domains.[7]

In mammals, NO is produced by three isoforms of NOS for diverse physiological functions.[1,2] The NO generated by the two constitutive isoforms, endothelial nitric oxide synthase (eNOS) and neuronal nitric oxide synthase (nNOS), is used as a messenger molecule for smooth muscle relaxation and for neurotransmission, respectively. Their activity is regulated by intracellular calcium levels, which control the electron transfer from the reductase to oxygenase domain via calmodulin binding. The NO produced by the inducible isoform, iNOS, which has calmodulin permanently bound,[7] is used for immunological protection. Overexpression of iNOS can cause the depletion of L-Arg and H_4B, leading to deleterious effects due to oxidative stress as a result of the release of the O_2 from NOS as superoxide via the uncoupled reaction.[8−10] The overproduction of NO itself may lead to various diseases characterized by acute and chronic inflammation, such as sepsis,[11] atherosclerosis,[12] transplant rejection,[13,14] asthma,[15] inflammatory bowel disease,[16] and arthritis.[17]

As NO production can be a double-edged sword, the activity of iNOS has to be tightly regulated. Accordingly, its expression is controlled by several cellular factors other than calcium-

[†] Albert Einstein College of Medicine.
[‡] The Cleveland Clinic.

(1) Alderton, W. K.; Cooper, C. E.; Knowles, R. G. *Biochem. J.* **2001**, *357*, 593–615.
(2) Li, H.; Poulos, T. L. *J. Inorg. Biochem.* **2005**, *99*, 293–305.
(3) Stuehr, D. J. *Biochim. Biophys. Acta* **1999**, *1411*, 217–230.
(4) Stuehr, D. J.; Kwon, N. S.; Nathan, C. F.; Griffith, O. W.; Feldman, P. L.; Wiseman, J. *J. Biol. Chem.* **1991**, *266*, 6259–6263.
(5) Crane, B. R.; Arvai, A. S.; Ghosh, D. K.; Wu, C.; Getzoff, E. D.; Stuehr, D. J.; Tainer, J. A. *Science* **1998**, *279*, 2121–2126.
(6) Kwon, N. S.; Nathan, C. F.; Stuehr, D. J. *J. Biol. Chem.* **1989**, *264*, 20496–20501.
(7) Spratt, D. E.; Israel, O. K.; Taiakina, V.; Guillemette, J. G. *Biochim. Biophys. Acta* **2008**, *1784*, 2065–2070.
(8) Bonomini, F.; Tengattini, S.; Fabiano, A.; Bianchi, R.; Rezzani, R. *Histol. Histopathol.* **2008**, *23*, 381–390.
(9) Cai, H.; Harrison, D. G. *Circ. Res.* **2000**, *87*, 840–844.
(10) Puddu, P.; Puddu, G. M.; Cravero, E.; Rosati, M.; Muscari, A. *Blood Pressure* **2008**, *17*, 70–77.
(11) Wong, J. M.; Billiar, T. R. *Adv. Pharmacol.* **1995**, *34*, 155–170.
(12) Dusting, G. J. *EXS* **1996**, *76*, 33–55.
(13) Smith, S. D.; Wheeler, M. A.; Zhang, R.; Weiss, E. D.; Lorber, M. I.; Sessa, W. C.; Weiss, R. M. *Kidney Int.* **1996**, *50*, 2088–2093.
(14) Pieper, G. M.; Roza, A. M. *Free Radical Biol. Med.* **2008**, *44*, 1536–1552.
(15) Batra, J.; Chatterjee, R.; Ghosh, B. *Indian J. Biochem. Biophys.* **2007**, *44*, 303–9.
(16) Kolios, G.; Valatas, V.; Ward, S. G. *Immunology* **2004**, *113*, 427–437.
(17) Cuzzocrea, S. *Curr. Pharm. Des.* **2006**, *12*, 3551–3570.

 10.1021/ja901016a CCC: $40.75

Scheme 1

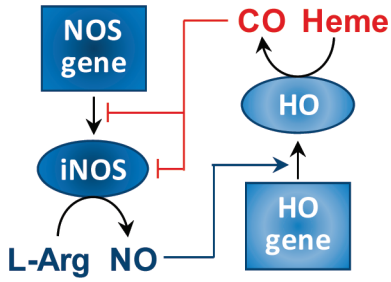

induced calmodulin binding.[18,19] In addition, NO produced by iNOS up-regulates the expression of heme oxygenase (HO), which in turn produces carbon monoxide (CO) that can down-regulate iNOS activity by reducing its expression level and by directly inhibiting the enzyme, as illustrated in Scheme 1.[20−22] On this basis, CO has been recognized as an important attenuator of inflammation.[23−25] Despite its importance, the molecular mechanism underlying the CO-induced inactivation of iNOS remains unclear.

NOSs belong to the P450 family of enzymes, with a negatively charged thiolate ligand, that is, a deprotonated cysteine, coordinated to the heme iron.[26] The binding of CO to iNOS, like other members of the P450 family, produces a species with a Soret band at ~450 nm ($iNOS_{P450}$),[27−29] which can spontaneously convert to an inactive "P420" species ($iNOS_{P420}$), characterized by a Soret band at ~420 nm.[30−33] It has been proposed that the P450 → P420 transition in the cytochrome P450 family of enzymes is associated with replacement of the native thiolate ligand by a histidine residue, on the basis of the following observations: (1) The optical absorption spectra of the P420s are similar to those of hemeproteins with a histidine as the proximal heme ligand, such as myoglobin (Mb).[34] (2) A Raman band at 218 cm^{-1} identified in the 10-ns photoproduct of the P420 form of cytochrome P450 was assigned as an iron−histidine stretching mode on the basis of its similarity to the photoproduct of a low-pH form of Mb.[35] (3) The equilibrium Raman spectra of the P420 derivatives of NOSs, P450s, and chloroperoxidase are similar to that of the low-pH form of Mb.[36] Although the evidence is compelling, in most of the enzymes, including iNOS, there are no histidine residues present within 10 Å of the heme iron; it is not obvious as to why and how CO binding could trigger such a large conformational change in different P450-type enzymes—with diverse sequences and structures—to bring a histidine residue in close proximity to the heme iron in an energetically feasible fashion.

In contrast, instead of ligand switching, other evidence suggests that the P450 → P420 transition is a result of the protonation of the thiolate ligand: (1) When CO adducts of porphyrin model complexes with a ferrous iron are coordinated by a thiolate ligand, they exhibit P450-type spectra, which convert to P420-type spectra when the thiolate ligand is protonated.[26,37] (2) In a cytochrome P450 from *Mycobacterium tuberculosis*, the P450 → P420 conversion is controlled by pH, with the P420 form preferred at low pH.[30]

The difficulty in characterizing the molecular properties of P420 lies in the fact that the CO adducts of neutral thiol- and imidazole-bound hemes display similar optical spectroscopic properties. The spectral similarity between the two types of CO adduct is surprising but is consistent with the prediction derived from extended Hückel calculations.[38] Along these lines, the CO adducts of the neutral thiol- and imidazole-bound H93G mutant of Mb exhibit similar MCD spectral patterns and intensities, which are akin to those of the CO adduct of the wild-type Mb.[39]

In this study, we used steady-state and time-resolved resonance Raman and optical absorption spectroscopic techniques to determine the identity of the proximal ligand of $iNOS_{P420}$ by comparing it to horse heart Mb and a CO derivative of a *n*-propanethiol-coordinated hemin dimethyl ester model complex. On the basis of the new data, we conclude that CO binding to the oxygenase domain of iNOS causes reversible protonation of the native thiolate anion proximal heme ligand to a neutral thiol, instead of switching to histidine as previously proposed.[35,36]

Materials and Methods

Hemin dimethyl ester was purchased from Porphyrin Products (Logan, UT). The natural-abundance CO and the $^{13}C^{18}O$ isotope were obtained from Tech Air (White Plains, NY) and Icon Isotopes (Summit, NJ), respectively. Lyophilized salt-free horse heart myoglobin and all other chemicals were from Sigma−Aldrich Corp. (St. Louis, MO). All the chemicals were used without further purification and were prepared with deionized water (Millipore). The oxygenase domain of murine iNOS was prepared as described elsewhere.[40] Briefly, the iNOSoxy gene with a C-terminal six-histidine tag was cloned into a pCWori vector. The protein was expressed in *Eshcerichia coli* and purified by using a Ni-NTA affinity column. The purified enzyme in 40 mM pH 7.6 *N*-(2-hydroxyethyl)piperazine-*N*′-3-propanesulfonic acid (EPPS) buffer with 1 mM dithiothreitol (DTT) was stored at 77 K until use. All the protein samples were prepared in 40 mM pH 7.6 EPPS buffer without DTT, except where indicated. To generate the CO adducts, the protein samples were first purged with CO gas under anaerobic

(18) Aktan, F. *Life Sci.* **2004**, *75*, 639–653.
(19) Korhonen, R.; Lahti, A.; Kankaanranta, H.; Moilanen, E. *Curr. Drug Targets: Inflammation Allergy* **2005**, *4*, 471–479.
(20) Kim, H. S.; Loughran, P. A.; Billiar, T. R. *Nitric Oxide* **2008**, *18*, 256–265.
(21) Srisook, K.; Han, S. S.; Choi, H. S.; Li, M. H.; Ueda, H.; Kim, C.; Cha, Y. N. *Biochem. Pharmacol.* **2006**, *71*, 307–318.
(22) True, A. L.; Olive, M.; Boehm, M.; San, H.; Westrick, R. J.; Raghavachari, N.; Xu, X.; Lynn, E. G.; Sack, M. N.; Munson, P. J.; Gladwin, M. T.; Nabel, E. G. *Circ. Res.* **2007**, *101*, 893–901.
(23) Abraham, N. G.; Kappas, A. *Pharmacol. Rev.* **2008**, *60*, 79–127.
(24) Piantadosi, C. A. *Free Radical Biol. Med.* **2008**, *45*, 562–9.
(25) Ryter, S. W.; Morse, D.; Choi, A. M. *Sci. STKE* **2004**, *2004*, RE6.
(26) Stern, J. O.; Peisach, J. *J. Biol. Chem.* **1974**, *249*, 7495–7498.
(27) Wang, J.; Stuehr, D. J.; Ikeda-Saito, M.; Rousseau, D. L. *J. Biol. Chem.* **1993**, *268*, 22255–22258.
(28) White, K. A.; Marletta, M. A. *Biochemistry* **1992**, *31*, 6627–6631.
(29) Sono, M.; Stuehr, D. J.; Ikeda-Saito, M.; Dawson, J. H. *J. Biol. Chem.* **1995**, *270*, 19943–19948.
(30) Dunford, A. J.; McLean, K. J.; Sabri, M.; Seward, H. E.; Heyes, D. J.; Scrutton, N. S.; Munro, A. W. *J. Biol. Chem.* **2007**, *282*, 24816–24824.
(31) Hui Bon Hoa, G.; McLean, M. A.; Sligar, S. G. *Biochim. Biophys. Acta* **2002**, *1595*, 297–308.
(32) Omura, T.; Sato, R. *J. Biol. Chem.* **1964**, *239*, 2370–2378.
(33) Yu, C.; Gunsalus, I. C. *J. Biol. Chem.* **1974**, *249*, 102–106.
(34) Antonini, E.; Brunori, M. *Hemoglobin and Myoglobin in Their Reactions with Ligands*; North Holland Publishing Company: Amsterdam, 1971.
(35) Wells, A. V.; Li, P.; Champion, P. M.; Martinis, S. A.; Sligar, S. G. *Biochemistry* **1992**, *31*, 4384–4393.
(36) Wang, J.; Stuehr, D. J.; Rousseau, D. L. *Biochemistry* **1995**, *34*, 7080–7087.
(37) Collman, J. P.; Sorrell, T. N. *J. Am. Chem. Soc.* **1975**, *97*, 4133–4134.
(38) Hanson, L. K.; Eaton, W. A.; Sligar, S. G.; Gunsalus, I. C.; Gouterman, M.; Connell, C. R. *J. Am. Chem. Soc.* **1976**, *98*, 2672–2674.
(39) Perera, R.; Sono, M.; Sigman, J. A.; Pfister, T. D.; Lu, Y.; Dawson, J. H. *Proc. Natl. Acad. Sci. U.S.A.* **2003**, *100*, 3641–3646.
(40) Ghosh, D. K.; Wu, C.; Pitters, E.; Moloney, M.; Werner, E. R.; Mayer, B.; Stuehr, D. J. *Biochemistry* **1997**, *36*, 10609–10619.

conditions, followed by reduction with a minimal amount of sodium dithionite. The protein concentration used for the equilibrium optical and Raman measurements was 40 μM; that for the photolysis measurements was 150 μM.

The CO adduct of the neutral thiol−heme model complex was prepared anaerobically by dissolving hemin dimethyl ester and sodium dithionite in a solvent mixture of water/benzene/*n*-propanethiol (with a volume ratio of 3:3:1), which was prepurged with CO. The solution mixture was shaken thoroughly for several minutes until the color of the organic layer, containing the neutral thiol−heme model complex, changed from brown to bright pink (the aqueous layer containing sodium dithionite remained colorless). The CO adduct of the neutral thiol−heme model complex residing in the organic layer was transferred with a Hamilton gastight syringe to an argon-purged optical cuvette or Raman rotating cell for absorption or Raman spectroscopic measurements, respectively.

The optical absorption spectra were obtained with a UV2100 spectrophotometer from Shimadzu Scientific Instruments, Inc. (Columbia, MD) with a spectral slit width of 1 nm. To measure the steady-state resonance Raman spectra, the 413.1 nm excitation from a Kr ion laser (Spectra Physics, Mountain View, CA) was focused to a ~30 μm spot on the spinning quartz cell rotating at ~1000 rpm. The scattered light, collected at a right angle to the incident laser beam, was focused on the 100 μm-wide entrance slit of a 1.25 m Spex spectrometer equipped with a 1200 grooves/mm grating (Horiba Jobin Yvon, Edison, NJ), where it was dispersed and then detected by a liquid nitrogen-cooled charge-coupled device (CCD) detector (Princeton Instruments, Trenton, NJ). A holographic notch filter (Kaiser, Ann Arbor, MI) was used to remove the laser line. The Raman shift was calibrated by using indene and an acetone/ferricyanide mixture for the 300−1700 and 1900−2000 cm^{-1} spectral windows, respectively. The laser power was kept <5 mW for all measurements to avoid photodissociation of the heme-bound CO. The spectral acquisition times for the ν_{Fe-CO} and ν_{C-O} measurements were ~30 and 120 min, respectively.

To obtain the spectrum of the photolyzed species of $iNOS_{P420}$, a 5-ns laser pulse (532 nm, 10 Hz) from a frequency-doubled Nd:YAG laser (Quantel Brilliant B; Big Sky Laser Technologies, Bozeman, MT) was used to generate a 435.7 nm line from a 1 m long hydrogen shifter (Light Age, Inc., Somerset, NJ) pressurized with H_2 gas at 150 psi. The 435.7 nm laser pulse was used to photodissociate the CO from the protein and at the same time was used as the excitation light source for the Raman measurement. The Raman spectrum was obtained with a 1 m focal length spectrometer (model 1000M, Spex Industries Inc., Edison, NJ) equipped with a CCD detector (Spectrum ONE from Instruments S.A. Inc., Edison, NJ). The averaged laser power and acquisition time were 5−6 mW and 7 h, respectively. The Mb sample in D_2O was prepared by dissolving lyophilized myoglobin in D_2O buffer. For iNOS, a 200 μL sample of ferric, substrate- and DTT-free iNOS in H_2O buffer was exchanged with 20 mL of D_2O buffer in an Amicon centrifugal filter device (Millipore). Both samples were stored at 4 °C for 12 h before data acquisition.

For the pH-dependent studies, 800 μL of 10 μM iNOS in 40 mM EPPS buffer, in the presence of either 2 mM DTT or 2 mM L-arginine, was purged with CO and reduced with excess dithionite. After the $iNOS_{P450} \rightarrow iNOS_{P420}$ conversion reaches the equilibrium state, the sample was titrated with HCl. The conversion from $iNOS_{P450}$ to $iNOS_{P420}$ was followed as a function of pH by optical absorption measurements.

Results and Discussion

As shown in Figure 1, immediately following CO binding to the L-Arg and H_4B-free iNOS, the enzyme exhibits a P450-type spectrum with a Soret band at 444 nm, a single visible band at 551 nm. Within a 5-h time window, it gradually converts to $iNOS_{P420}$, with a Soret band at 420 nm and visible bands at 539 and 568 nm. Extended incubation (~12 h) leads to almost

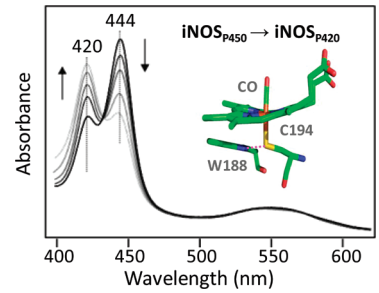

Figure 1. Spontaneous conversion of $iNOS_{P450}$ to $iNOS_{P420}$. Time-dependent spectra were obtained following exposure of reduced iNOS to CO in the absence of L-Arg and H_4B in pH 7.6 EPPS buffer without DTT within a time window of 5 h. (Inset) Crystal structure of the CO adduct of iNOS in the presence of L-Arg and H_4B (PDB code 2G6M).

complete conversion to the $iNOS_{P420}$ species (vide infra). Upon exposure to air, the $iNOS_{P420}$ species spontaneously oxidizes to the native ferric form (data not shown). As a deoxy species was not observed during the reaction, the reaction appears to be rate-limited by CO dissociation. The ferric enzyme thus produced can be rereduced and coordinated by CO to regenerate the active P450 form. The process can be repeated several times without sacrificing the integrity of the enzyme as reported by Abu-Soud et al.[41] The data demonstrate that the change in the proximal ligand associated with the $iNOS_{P450} \rightarrow iNOS_{P420}$ conversion is a reversible process and that the native proximal ligand of the enzyme is thermodynamically favored in the ferric state.

The presence of L-Arg or H_4B partially inhibits the $iNOS_{P450} \rightarrow iNOS_{P420}$ conversion (vide infra), whereas the presence of both L-Arg and H_4B completely prevents the transition. It is well-established that the substrate- and cofactor-free iNOS exists as a "loose" dimer. The binding of L-Arg or H_4B promotes its partial conversion to a "tight" dimer, which exhibits increased resistance toward proteolytic cleavage[40] and detergent-induced dissociation of dimer into monomers,[42−44] while the presence of both L-Arg and H_4B leads to a complete conversion to the "tight" dimer. The conformational stability afforded by the "tight" dimer in L-Arg- or H_4B-bound enzyme presumably accounts for the partial inhibition of the $iNOS_{P420}$ formation. The data indicate that the $iNOS_{P450} \rightarrow iNOS_{P420}$ transition is related to the "tight" dimer ↔ "loose" dimer equilibrium.

Like L-Arg, the presence of DTT partially inhibits the $iNOS_{P450} \rightarrow iNOS_{P420}$ conversion. DTT has been shown to be a competitive inhibitor of L-Arg binding to nNOS.[45,46] The inhibition effect of DTT against $iNOS_{P420}$ formation can hence be attributed to the occupation of the DTT molecule in the L-Arg binding site, thereby affecting the "tight" dimer ↔ "loose" dimer equilibrium.

In the absence of DTT, L-Arg, and H_4B, pH-dependent studies show that the $iNOS_{P450} \rightarrow iNOS_{P420}$ conversion reaches completion independent of the pH (between 6.9 and 8.9), whereas in the presence of L-Arg or DTT the conversion is pH-sensitive.

(41) Abu-Soud, H. M.; Wu, C.; Ghosh, D. K.; Stuehr, D. J. *Biochemistry* **1998**, *37*, 3777–3786.
(42) Abu-Soud, H. M.; Loftus, M.; Stuehr, D. J. *Biochemistry* **1995**, *34*, 11167–11175.
(43) Klatt, P.; Schmidt, K.; Lehner, D.; Glatter, O.; Bachinger, H. P.; Mayer, B. *EMBO J.* **1995**, *14*, 3687–3695.
(44) Rodriguez-Crespo, I.; Gerber, N. C.; Ortiz de Montellano, P. R. *J. Biol. Chem.* **1996**, *271*, 11462–11467.
(45) McMillan, K.; Masters, B. S. S. *Biochemistry* **1993**, *32*, 9875–9880.
(46) Gorren, A. C.; Schrammel, A.; Schmidt, K.; Mayer, B. *Biochemistry* **1997**, *36*, 4360–4366.

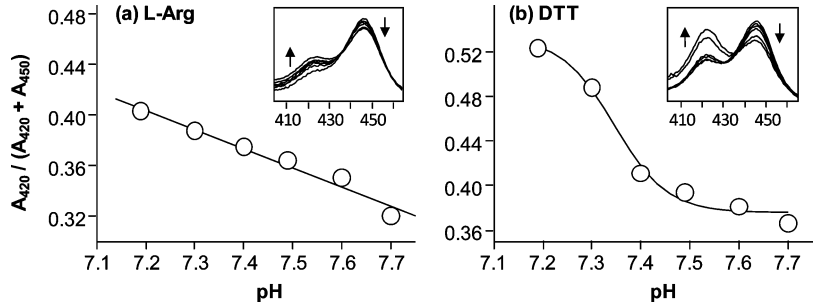

Figure 2. pH-dependent $iNOS_{P450} \rightarrow iNOS_{P420}$ conversion in the presence of (a) 2 mM L-Arg or (b) 2 mM DTT. The *y*-axis is determined by $A_{420}/(A_{420} + A_{450})$, where A_{420} and A_{450} stand for the absorbance of the $iNOS_{P420}$ and $iNOS_{P450}$ forms measured at 420 and 444 nm, respectively. (Insets) pH-dependent absorbance spectra.

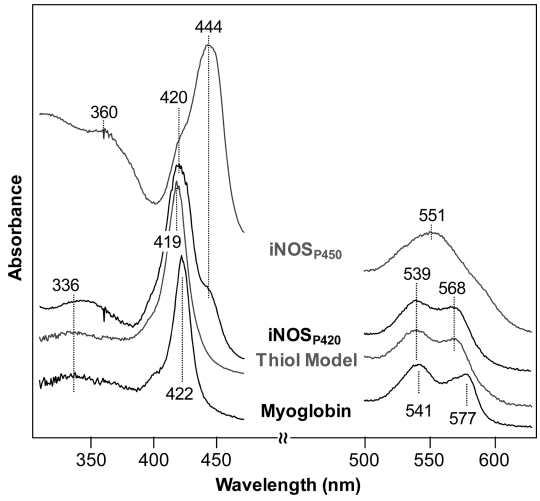

Figure 3. Optical absorbance spectra of CO derivatives of $iNOS_{P450}$, $iNOS_{P420}$, myoglobin, and a neutral thiol−heme complex. The $iNOS_{P450}$ sample was prepared as described in Figure 1, while the $iNOS_{P420}$ species was obtained after a 12 h incubation of the $iNOS_{P450}$ sample. The model complex was generated by binding CO and *n*-propanethiol to hemin dimethyl ester.

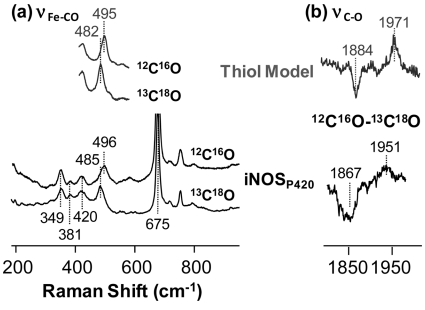

Figure 4. Resonance Raman spectra of CO adducts of $iNOS_{P420}$ and the neutral thiol−heme complex. The ν_{Fe-CO} modes were identified in the low-frequency region of the spectrum by comparing spectra of the $^{12}C^{16}O$- and $^{13}C^{18}O$-bound complexes as indicated in panel a. The ν_{C-O} modes were identified in the high-frequency region of the spectrum by the same isotope substitution experiments, as indicated by the $^{12}C^{16}O - {}^{13}C^{18}O$ difference spectra shown in panel b.

As shown in Figure 2, in the presence of DTT at pH 7.2, ~52% of $iNOS_{P420}$ was observed, which decreased to ~36% as pH increased to 7.7 in a sigmoidal fashion. The data indicate that the conformational change associated with the $iNOS_{P450} \rightarrow iNOS_{P420}$ transition in the presence of DTT is associated with an apparent pK_a of ~7.35. In contrast, in the presence of L-Arg at pH 7.2, ~40% of $iNOS_{P420}$ was observed, which linearly decreased to ~32% as pH increased to 7.7. The linear behavior may reflect the post-transition region of the pH-dependent conformational change associated with a lower pK_a value in the presence of L-Arg, as compared to DTT, as the percentage change (40−32%) is similar to that observed in the post-transition region of the DTT data. Unfortunately, the pH-dependent data at pH <7.2, which could test this hypothesis, were not detectable as the protein started to aggregate due to the instability of the protein structure at low pH. In summary, the data indicate that the $iNOS_{P450} \rightarrow iNOS_{P420}$ transition is coupled to the "tight" dimer ↔ "loose" dimer equilibrium and that the equilibrium is sensitive to the pH.

P420 Model Analogues. To determine whether the $iNOS_{P450} \rightarrow iNOS_{P420}$ transition is a result of ligand switching from a thiolate to a histidine or the protonation of the thiolate ligand, the electronic transition properties of $iNOS_{P420}$ with respect to a neutral thiol−heme model complex, CO-bound *n*-propanethiol hemin dimethyl ester, and CO-bound horse heart Mb were examined. The $iNOS_{P420}$ spectrum was obtained following a ~12 h incubation of the L-Arg and H_4B-free $iNOS_{P450}$ sample and compared to that of the neutral thiol−heme model complex. As shown in Figure 3, the optical absorption spectrum of the neutral thiol−heme complex is nearly identical to that of the $iNOS_{P420}$ complex with absorption maxima at 419, 539, and 568 nm, which are distinct from those of Mb at 422, 541, and 577 nm. As a comparison, the initial $iNOS_{P450}$ spectrum is also shown with its 444 nm Soret band, broad visible absorption band at 551 nm, and a red-shifted UV component compared to the other spectra. The $iNOS_{P420}$ spectrum is also distinguishable from that of a negatively charged thiolate model heme complex (formed by mixing CO, a thiolate, and the diethyl ester of Fe-protoporphyrin IX) with a Soret maximum at 449 nm[37] and from that of a bis-CO heme model complex (formed by mixing CO with hemin dimethyl ester) with a Soret maximum at 408 nm as reported[47] (data not shown). The optical absorption data are consistent with the assignment of a neutral thiol as the proximal heme ligand in the $iNOS_{P420}$ complex as a result of protonation of the native thiolate ligand.

CO-Related Vibrational Modes. To further investigate the nature of the proximal ligand of the $iNOS_{P420}$ species, we examined its resonance Raman spectrum. As shown in Figure 4, the ν_{C-O} and ν_{Fe-CO} modes of $iNOS_{P420}$ are present at 1951 and 496 cm^{-1}, respectively, in contrast to the 1946 and 491 cm^{-1} modes observed in native $iNOS_{P450}$.[48] In the difference

(47) Rougee, M.; Brault, D. *Biochem. Biophys. Res. Commun.* **1973**, *55*, 1364–1369.
(48) Rousseau, D. L.; Li, D.; Couture, M.; Yeh, S. R. *J. Inorg. Biochem.* **2005**, *99*, 306–323.

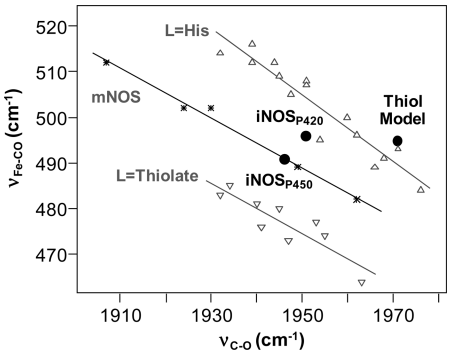

Figure 5. ν_{Fe-C} vs ν_{C-O} inverse correlation lines of mammalian NOS isoforms (mNOS), P450 enzymes (L = thiolate), and histidine-ligated enzymes (L = His). Data points associated with active iNOS (iNOS$_{P450}$), iNOS$_{P420}$, and heme−thiol model complex are as indicated. The remaining data points are from refs 50−52 and references therein.

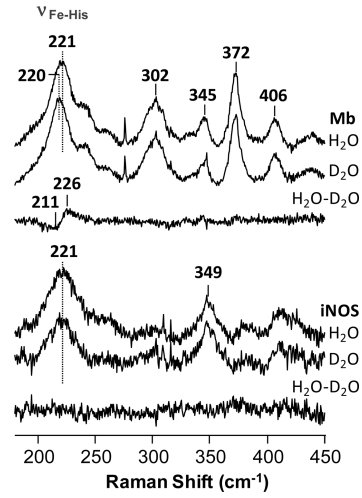

Figure 6. Time-resolved resonance Raman spectra of 5-ns photoproducts of myoglobin (top) and iNOS$_{P420}$ (bottom) in H_2O vs D_2O. The H_2O − D_2O isotope difference spectra are as indicated. The acquisition time for each spectrum was 7 h.

spectra shown in Figure 4b, all the heme modes are canceled out and the remaining positive and negative peaks are associated with the $^{12}C-^{16}O$ and $^{13}C-^{18}O$ stretching modes, respectively. As a comparison, the CO adduct of the neutral thiol−heme model complex was also examined. The Raman spectrum of the model complex shows that the ν_{C-O}/ν_{Fe-CO} modes are at 1971 and 495 cm^{-1} (Figure 4).

The ν_{C-O} and ν_{Fe-CO} modes typically follow an inverse correlation, reflecting the electrostatic environment of the heme-bound CO due to the resonance between the following two extreme structures of the L−Fe−CO moiety (where L is the proximal heme iron ligand).[49]

$$L-Fe^{\delta-}-C\equiv O^{\delta+} \leftrightarrow L-Fe=C=O$$

On the other hand, the offset of the inverse correlation line in the ν_{C-O} versus ν_{Fe-CO} plot is determined by the electronic properties of the proximal heme ligand (L). The data from several enzyme systems with thiolate and histidine as proximal ligands are presented in Figure 5.[50−52] Hemeproteins with His as a proximal ligand stay on a line lying above the P450 line, constructed by the data from enzymes with a more electron-donating thiolate as the proximal ligand. The mammalian NOS (mNOS) line lies between the histidine and the thiolate line, as the proximal thiolate ligand in iNOS accepts an H-bond from a nearby tryptophan residue (see W188 in iNOS shown in Figure 1), which reduces the electron-donating capability of the thiolate ligand. Interestingly, the iNOS$_{P450}$ data point is positioned directly on the mNOS line, while the iNOS$_{P420}$ data point lies above the mNOS line, consistent with the proposal that its proximal ligand is a protonated thiol, which is expected to donate less electron density to the heme iron as compared to that in the active iNOS$_{P450}$ species. The data point associated with the neutral thiol−heme model complex is positioned above the thiolate correlation line (Figure 5), also in agreement with the expected weaker electron donation from its neutral thiol proximal ligand. The horizontal displacement of the ν_{C-O} of the neutral thiol−heme model complex from the iNOS$_{P420}$ data in the correlation plot is plausibly a result of (1) the strain imposed by the protein matrix on the proximal ligand in the latter, (2) differences in the orientation of the proximal ligand, or (3) the protonation state of the propionates, as proposed for other heme protein systems.[53] These changes can cause horizontal displacement of the ν_{C-O} mode while leaving ν_{Fe-CO} unaffected.

It is important to note that several heme out-of-plane modes observed in the low-frequency region of the spectrum of the native iNOS$_{P450}$, such as those at 693, 734, and 803 cm^{-1},[54] are absent in the spectrum of the iNOS$_{P420}$ shown in Figure 4a, indicating that the distorted heme in the native iNOS$_{P450}$ became planar when it converted to the P420 form. Likewise, the ν_2 mode of heme proteins was shown by Czernuszewicz et al.[55] to be sensitive to heme distortion based on the studies of nickel octaethylporphyrin model complexes. In iNOS$_{P450}$, it is observed at 1573 cm^{-1}, whereas it is observed at 1581 cm^{-1} in iNOS$_{P420}$,[36] consistent with a more planar heme in iNOS$_{P420}$.

5-ns Photoproduct of iNOS$_{P420}$. To directly examine the iron−proximal ligand stretching mode, the 5-ns time-resolved resonance Raman spectrum of the photolysis product of iNOS$_{P420}$ was measured. As shown in Figure 6, the photoproduct of iNOS$_{P420}$ (in which CO is photolyzed) displays a strong band at 221 cm^{-1}, similar to that of the P420 derivative of a cytochrome P450.[35] This band is not present in the six-coordinate CO-bound form of iNOS$_{P420}$ (Figure 4) or in the 5-ns photolysis product of the active iNOS$_{P450}$, in either the presence or absence of L-Arg and H_4B (data not shown). The frequency of this mode is similar to that of the iron−histidine stretching mode (ν_{Fe-His}) of myoglobin[56] and is 117 cm^{-1} lower than the iron−thiolate stretching frequency,[57] in line with the expected weaker iron−thiol bond, suggesting that it can be either a ν_{Fe-His} mode or iron−thiol stretching mode (ν_{Fe-SH}). To test it, we

(49) Spiro, T. G.; Wasbotten, I. H. *J. Inorg. Biochem.* **2005**, *99*, 34–44.
(50) Song, S.; Boffi, A.; Chiancone, E.; Rousseau, D. L. *Biochemistry* **2002**, *32*, 6330.
(51) Wang, J.; Takahashi, S.; Rousseau, D. L. *Proc. Natl. Acad. Sci. U.S.A.* **1995**, *92*, 9402–9406.
(52) Yu, N.-T.; Kerr, E. A. In *Biological Applications of Raman Spectroscopy*; Spiro, T. G., Ed.; John Wiley & Sons: New York, 1988; Vol. III, pp 39−95.
(53) Xu, C.; Ibrahim, M.; Spiro, T. G. *Biochemistry* **2008**, *47*, 2379–87.
(54) Li, D.; Stuehr, D. J.; Yeh, S. R.; Rousseau, D. L. *J. Biol. Chem.* **2004**, *279*, 26489–26499.
(55) Czernuszewicz, R. S.; Li, X. Y.; Spiro, T. G. *J. Am. Chem. Soc.* **1989**, *111*, 7024–7031.
(56) Argade, P. V.; Sassardi, M.; Rousseau, D. L.; Inubushi, T.; Ikeda-Saito, M.; Lapidot, A. *J. Am. Chem. Soc.* **1984**, *106*, 6593–6596.
(57) Santolini, J.; Roman, M.; Stuehr, D. J.; Mattioli, T. A. *Biochemistry* **2006**, *45*, 1480–1489.

examined the H_2O-D_2O solvent isotope effect of the 221 cm^{-1} mode of $iNOS_{P420}$, as compared to that of the ν_{Fe-His} mode of Mb.

By use of a simple diatomic oscillator model, the expected shifts for replacing the labile proton with deuterium can be calculated by taking the square root of the ratio of the reduced masses of the deuterated and undeuterated species coordinated to the iron atom (mass = 56). In the case of the imidazole moiety (mass = 67) and the sulfur (mass = 32) of the thiol, the calculated shifts of an Fe−ligand mode at 221 cm^{-1} are 0.7 and 2 cm^{-1}, respectively. As shown in Figure 6, for Mb, a down-shift in the ν_{Fe-His} frequency was observed in D_2O. The H_2O-D_2O isotopic shift was calculated to be 1.5 cm^{-1} by the method reported previously,[58] with the assumption that the ν_{Fe-His} mode can be described by a Gaussian function.[59] The same experiment was performed with $iNOS_{P420}$, but no isotopic shift was detected for the analogous 221 cm^{-1} mode. Thus, the data indicate that the 221 cm^{-1} mode is neither a ν_{Fe-His} nor a ν_{Fe-SH} mode; instead it is likely a heme mode that is enhanced when a neutral thiol binds to the heme iron. The absence of a ν_{Fe-His} mode in the spectrum of the photolyzed $iNOS_{P420}$ excludes the possibility that the $iNOS_{P450} \rightarrow iNOS_{P420}$ transition is associated with ligand switching of the native thiolate with a histidine. It could be argued that in iNOS the histidine did not become deuterated, reflecting the lack of a detectable shift. However, the "nearby" histidines (>10 Å) are solvent-accessible and would likely be readily deuterated. Furthermore, we would expect increased solvent accessibility in the "loose" conformation.

It is noteworthy that we attempted to detect the ν_{Fe-SH} mode of the photoproduct of the neutral thiol−heme complex but, upon photolysis, the complex converted to a four-coordinate state instead of a five-coordinate complex (data not shown). A plausible explanation for why the five-coordinate structure was detectible in iNOS and Mb within 5 ns and not in the model complex is that the protein matrix plays an important role in keeping the proximal ligand close to the heme. In an aqueous study of histidine and CO binding to chlorohemin, there is little ligand recombination between 10 ps and 100 ns,[60] and the histidine does not bind until an H_2O−heme−CO complex forms because the histidine has a much lower affinity for unliganded heme than for a CO-coordinated heme.[61] In the case of enzymes, however, the proximal ligand is held close to the heme iron, facilitating ligation.

Conclusions

Our data show that the low-frequency mode of the photoproduct of $iNOS_{P420}$ at ~221 cm^{-1} does not have an H_2O-D_2O solvent isotope shift as found in the genuine ν_{Fe-His} mode of Mb, indicating that it is neither a ν_{Fe-His} nor a ν_{Fe-SH} mode. It confirms that the proximal ligand of $iNOS_{P420}$ is not a histidine. The ν_{Fe-CO} and ν_{C-O} data reveal that the proximal heme ligand of $iNOS_{P420}$ is consistent with a protonated thiol instead of a thiolate anion. In addition, the optical absorption properties of $iNOS_{P420}$ are similar to those of a neutral thiol−heme model complex instead of Mb, indicating that the proximal ligand of $iNOS_{P420}$ is a protonated thiol.

Thiols in free solution typically exhibit pK_a values between 8 and 10. The cysteine side chain, for example, has a pK_a of 8.2, but when incorporated into peptides, the pK_a can be as low as 7.4.[62] Additionally, upon coordination to a heme iron, the pK_a of the cysteine side chain could be further perturbed, as the positive charge of the ferric iron would stabilize a negatively charged thiolate. For instance, ethanethiol with a pK_a of ~10.5 in free solution[63] is *deprotonated* when bound to the H93G cavity mutant of sperm whale Mb in pH 7 aqueous solution.[64] Upon reduction of the heme iron to the ferrous state, the pK_a of thiolate ligands is increased due to the increase in the electron density on the iron, which increases the basicity of the thiolate anion; as a result, depending on the protein structure, the thiol may either bind to the heme iron as a protonated form (neutral thiol)[39] or totally lose its ligation.[64]

In the native $iNOS_{P450}$, the proximal thiolate ligand accepts a H-bond from W188 (Figure 1), which reduces the electron-donating capability of the thiolate, thereby stabilizing the ferrous iron−thiolate bond. Our data suggest that the $iNOS_{P450} \rightarrow iNOS_{P420}$ transition is associated with the protonation of the thiolate ligand rather than ligand switching with a histidine. The pH-dependent protonation of the thiolate ligand is concurrent with the breakage of the H-bonding interaction between W188 and the proximal thiolate ligand. For the L-Arg- and H_4B-free enzyme, the pK_a for the pH-dependent transition in the presence of DTT is ~7.35, which could reflect the pK_a of the proximal thiolate ligand.

While the full molecular basis for the $iNOS_{P450} \rightarrow iNOS_{P420}$ transition remains to be further explored, it is noteworthy that $iNOS_{P420}$ has a more planar heme, with the heme substituents oriented in distinct conformations as compared to the native enzyme. Our data suggest that this conformational change to the heme induced by CO binding to the substrate- and cofactor-free enzyme modifies the protein matrix, thereby shifting the "tight" dimer ↔ "loose" dimer equilibrium, disrupting the H-bond between the proximal thiolate ligand and W188, and allowing the entrance of water into the heme pocket to protonate the thiolate ligand to a neutral thiol.

The data demonstrate that the $iNOS_{P450} \rightarrow iNOS_{P420}$ transition is controlled by the conformational state of the enzyme. In the substrate- and cofactor-bound state, the enzyme is in the "tight" dimer conformation and unable to convert to $iNOS_{P420}$. With only L-Arg bound, the "tight" dimer ↔ "loose" dimer equilibrium shifts toward the "loose" dimer state; it hence is slightly more prone to $iNOS_{P420}$ formation. With DTT bound in the L-Arg binding site, the equilibrium shifts even more toward the "loose" dimer state, accounting for its higher preference for the $iNOS_{P420}$ form. In the absence of L-Arg and DTT, the enzyme is most susceptible to $iNOS_{P420}$ formation at all pH values tested, as the equilibrium completely shifts to the "loose" dimer state.

The importance of the protonation state of sulfur on the reactivity of thiolate-coordinated model complexes has been studied theoretically by density functional theory (DFT) calculations and experimentally by sulfur K-edge X-ray absorption spectroscopy recently.[65] Likewise, the H-bonding to the thiolate ligand in iNOS has been recognized to be

(58) Rousseau, D. L. *J. Raman Spectrosc.* **1981**, *10*, 94–99.
(59) Ondrias, M. R.; Rousseau, D. L.; Simon, S. R. *Proc. Natl. Acad. Sci. U.S.A.* **1982**, *79*, 1511–1514.
(60) Huang, Y.; Marden, M. C.; Lambry, J. C.; Fontaine-Aupart, M. P.; Pansu, R.; Martin, J. L.; Poyart, C. *J. Am. Chem. Soc.* **1991**, *113*, 9141–9144.
(61) Rougee, M.; Brault, D. *Biochemistry* **1975**, *14*, 4100–4106.
(62) Bulaj, G.; Kortemme, T.; Goldenberg, D. P. *Biochemistry* **1998**, *37*, 8965–8972.
(63) Kreevoy, M. M.; Harper, E. T.; Duvall, R. E.; Wilgus, H. S.; Ditsch, L. T. *J. Am. Chem. Soc.* **1960**, *82*, 4899–4902.
(64) Roach, M. P.; Pond, A. E.; Thomas, M. R.; Boxer, S. G.; Dawson, J. H. *J. Am. Chem. Soc.* **1999**, *121*, 12088–12093.
(65) Dey, A.; Okamura, T. A.; Ueyama, N.; Hedman, B.; Hodgson, K. O.; Solomon, E. I. *J. Am. Chem. Soc.* **2005**, *127*, 12046–12053.

important in controlling the oxygen chemistry performed by the enzyme and in regulating the NO-linked self-inhibition.[48] Here we show that the protonation of the thiolate ligand associated with the $iNOS_{P450} \rightarrow iNOS_{P420}$ transition plays a key role in the CO-linked inhibition mechanism of iNOS, underscoring the importance of proximal control in the NOS family of enzymes. Under conditions of chronic inflammation, such as atherosclerosis, when iNOS is highly expressed, the substrate and cofactor may be depleted. Consequently, the O_2 bound to the heme iron can be released as superoxide, which leads to the formation of a hydroxyl radical and other reactive oxygen species, thereby causing oxidative stress. The CO-induced inactivation of iNOS mediated by heme oxygenase (Scheme 1) is hence physiologically imperative for preventing the detrimental uncoupled reaction.

Acknowledgment. This work is supported by NIH Grants GM54806 to D.L.R., F31GM078679 to J.S., and CA53914, GM51491, and HL76491 to D.J.S.

JA901016A